

# PHASE TRANSITIONS IN POLYMERIC AND MICELLAR SYSTEMS

## 1. INTRODUCTION

The most active Small-Angle Neutron Scattering (SANS) research areas are in “Polymers” and “Complex Fluids” which include micellar systems. Understanding the thermodynamics of mixing of polymers and/or complex fluids is important. This involves insight into the major phase transitions and the various structures that are formed.

Polymer mixtures comprise polymer solutions, polymer blends, copolymers as well as their mixtures. Micelles are formed when a surfactant, oil and water are mixed. Adding oil forms a microemulsion. These systems form structures in the nanometer length scale that can be investigated by the SANS technique.

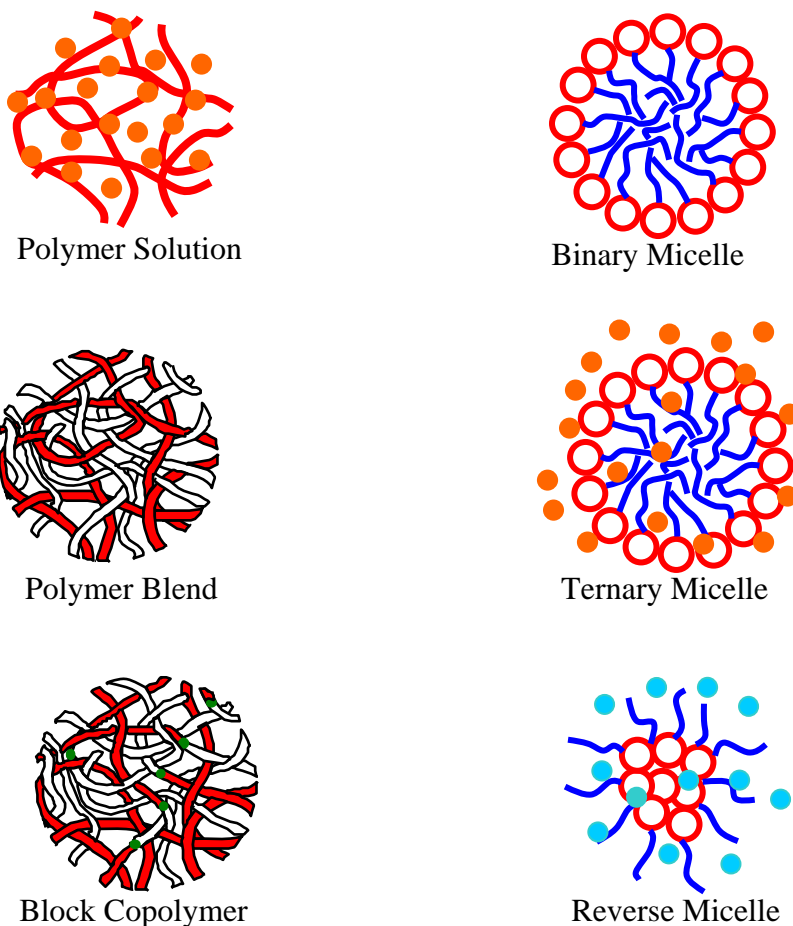


Figure 1: Various polymeric and micellar systems. The small dots represent solvent molecules.

## 2. PHASE TRANSITION BASICS

Polymer mixtures phase separate either through cooling and are characterized by an Upper Critical Spinodal Temperature (UCST), or upon heating and are characterized by a Lower Critical Spinodal Temperature (LCST). Combinations of LCST and UCST are also possible.

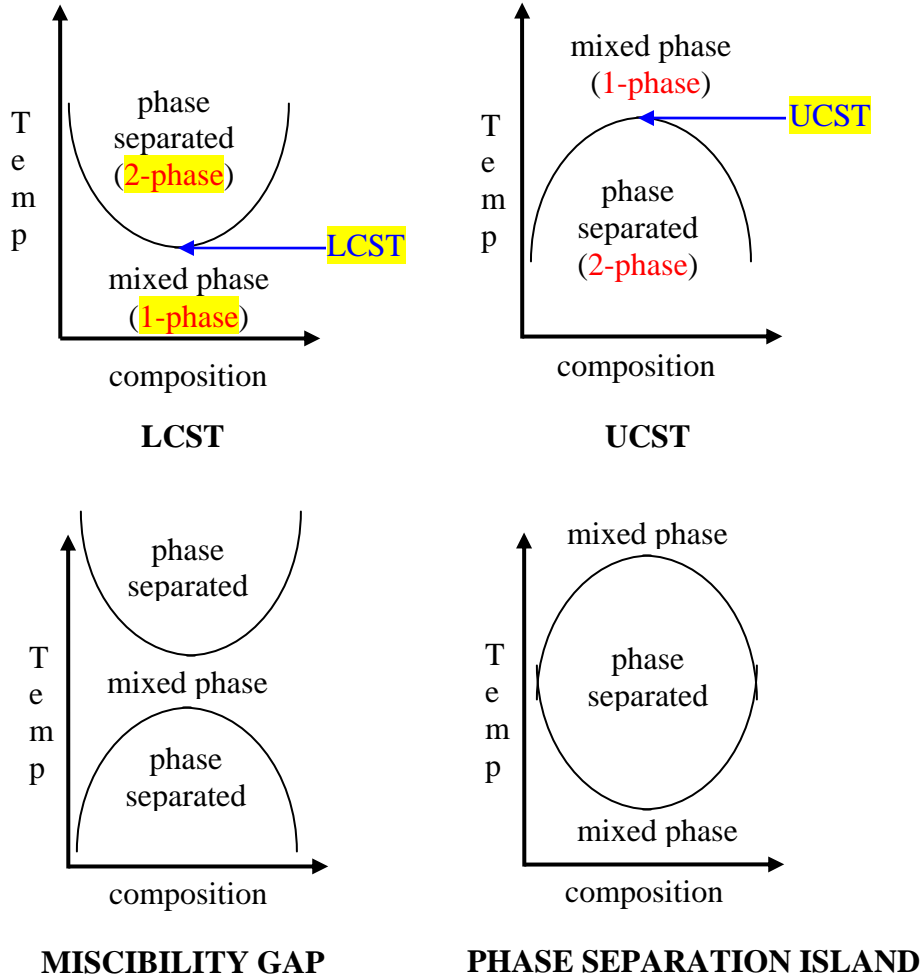


Figure 2: Various possible phase diagrams.

Composition fluctuations are enhanced when phase transition lines are approached from the mixed (1-phase) region. This increases the SANS intensity thereby making this technique an appropriate probe for thermodynamic (phase transition) studies.

The "binodal" condition is the phase transition line between the homogeneously mixed 1-phase region and the phase separated (i.e., demixed) 2-phase region in the temperature-composition phase diagram. The spinodal line is the deeper part of the demixed 2-phase region. The region between the binodal and the spinodal lines is the nucleation-and-growth region while the region within the spinodal line is called the spinodal region. Most water-soluble systems phase separate upon heating due to the softening of hydrogen-bonding at elevated temperatures. Note that the binodal line is mapped out

using **light scattering** (cloud point measurements) whereas the **spinodal line** is measured using **SANS**.

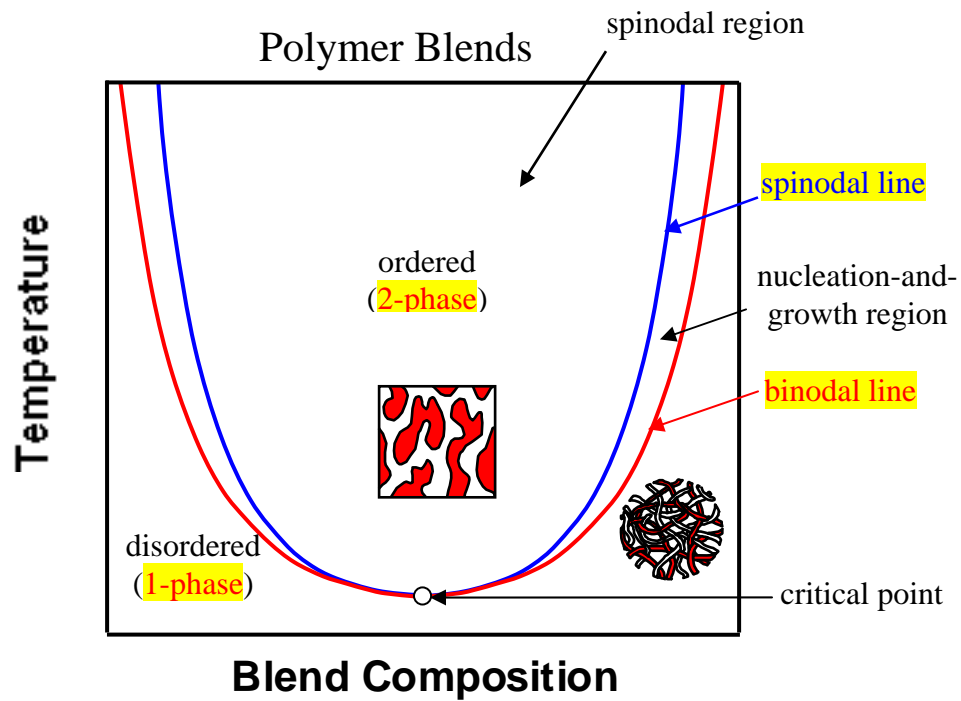


Figure 3: Schematic representation of the **phase diagram for an LCST polymer blend**.

For **block copolymers**, the **spinodal line** is referred to as the **Order-Disorder-Temperature (ODT)**. The ODT defines a region which comprises **three main forms of microphase separation**; these correspond to **spherical, cylindrical and lamellar morphologies**. The LCST line is referred to as the **Lower Critical Ordering Temperature (LCOT)** for copolymers. The copolymer composition is varied by increasing the length of one of blocks in the copolymer.

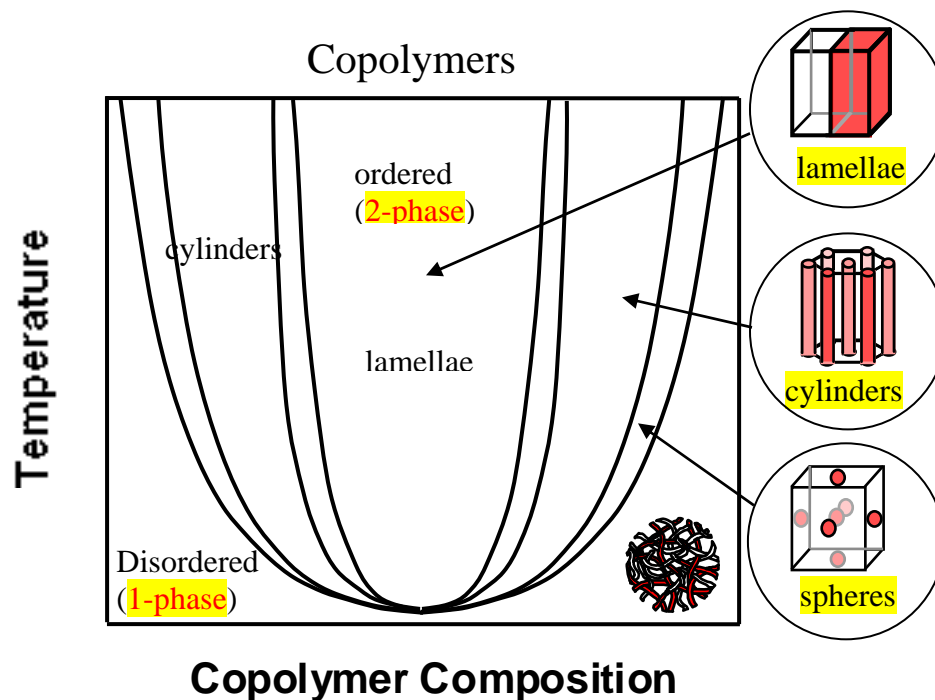


Figure 4: Representation of the various copolymer microphases for a Lower Critical Ordering Temperature (LCOT) system.

Surfactants are amphiphilic molecules which contain a hydrophilic part and a hydrophobic part. Surfactants can be ionic when the hydrophilic part of the molecule is charged. They can also be nonionic when the molecule is completely uncharged. When surfactants are mixed with water and are above a certain concentration and temperature, they form micelles in solution. The concentration threshold is called the Critical Micelle Concentration (CMC) and the temperature threshold is the Critical Micelle Temperature (CMT). One example of a nonionic surfactant is a Pluronic copolymer described next.

### 3. WHAT ARE PLURONICS?

Poly(ethylene oxide) (referred to as PEO) is the simplest water soluble polymer with a monomer structure  $-\text{CH}_2\text{CH}_2\text{O}-$ . Its neighbor in the homologous series poly(propylene oxide) (or PPO) does not dissolve in water at ambient temperature. Pluronics are triblock copolymers composed of one central PPO block connected to two PEO blocks. The PEO block dissolves well in aqueous media because it is mostly hydrophilic, while the PPO block does not dissolve because it is mostly hydrophobic at ambient temperature. This amphiphilic nature of pluronic molecules makes them form micelles at ambient temperature. At low temperature, this balance does not hold and both PEO and PPO blocks dissolve in water thereby remaining individual in the “unimers” phase (dissolved molecules). Pluronics are commercially available materials used in the cosmetics and pharmaceutical industries. The CMT and CMC vary depending on the block composition of the various pluronics which allows selection of the optimal surfactant for the desired application. The P85 pluronic considered here consists of 26 EO monomers in each of the

outside blocks and 40 PO monomers in the middle block. P85 is referred to as  $\text{EO}_{26}\text{PO}_{40}\text{EO}_{26}$ . The molecular weight of P85 is around 4,600 g/mol.

#### 4. SANS FROM P85 PLURONIC

The interest here is in micelle-formation as well as in the investigation of phase transitions that form various microstructures. A couple of P85 samples of different weight fractions in  $\text{D}_2\text{O}$  (d-water) were prepared and measured by SANS.

In order to investigate micelle formation, SANS data were taken from 10 % by weight P85 in deuterated water (d-water) at various temperatures (from 10 °C to 60 °C). Deuterated water was used in order to enhance the neutron contrast. Micelles are well formed at 30 °C. When micelles are formed, the scattering is characterized by two features: a peak characteristic of inter-micelles interactions, and decay at high Q characterizing the tail of the single-particle form factor. In-between these two features, a second shoulder (around  $Q = 0.15 \text{ \AA}^{-1}$ ) can be observed. This shoulder is also characteristic of the single particle form factor (oscillation of the spherical Bessel function) and is more or less visible depending on the size polydispersity of the micelles.

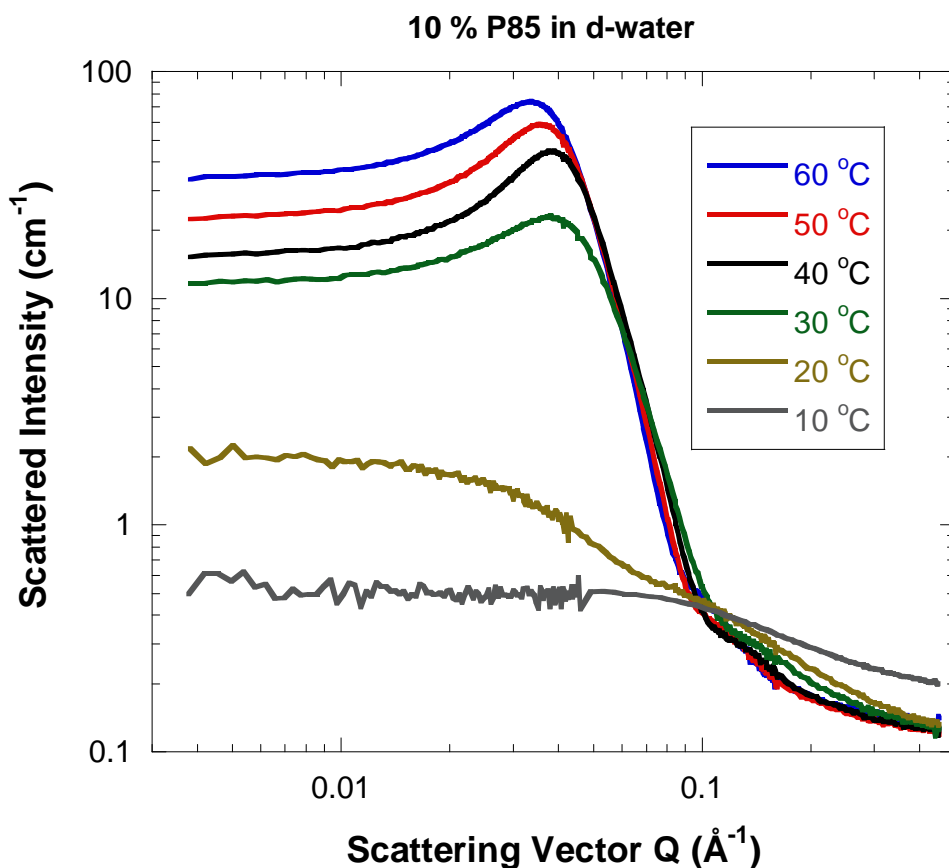


Figure 5: SANS data from the 10 % by weight P85 in  $\text{D}_2\text{O}$  at various temperatures. Data statistics are different for the two (low-Q and high-Q) instrument configurations. The overlap region for the two SANS configurations used is around  $0.04 \text{ \AA}^{-1}$ .

SANS data are shown also for a 0.5 % by weight P85/d-water sample for a wider temperature range (10 °C to 100 °C). The low P85 weight fraction allows the observation of single-particle effect (form factor) without interference from the inter-particle interaction peak. The intensity is seen to increase with increasing temperature but the shape of the form factor changes from unimers (below the CMT) to spherical micelles, then to cylindrical micelles and finally to lamellar micelles. This is a rich phase behavior and structural transitions which are deduced based on standard clues in the SANS spectra.

Scattering for unimers (low temperature) is characterized by a  $1/Q^2$  variation in the high-Q (so-called Porod) region. Spherical and cylindrical micelles are characterized by a  $1/Q^4$  variation in the Porod region. Cylindrical micelles are also characterized by a  $1/Q$  variation in the low-Q region (rod-like scattering). Lamellae are characterized by a  $1/Q^2$  dependence in the low-Q region (scattering from a 2D object) and the formation of an inter-lamellar Bragg peak for the highest temperature. This last structure is a demixed lamellae phase.

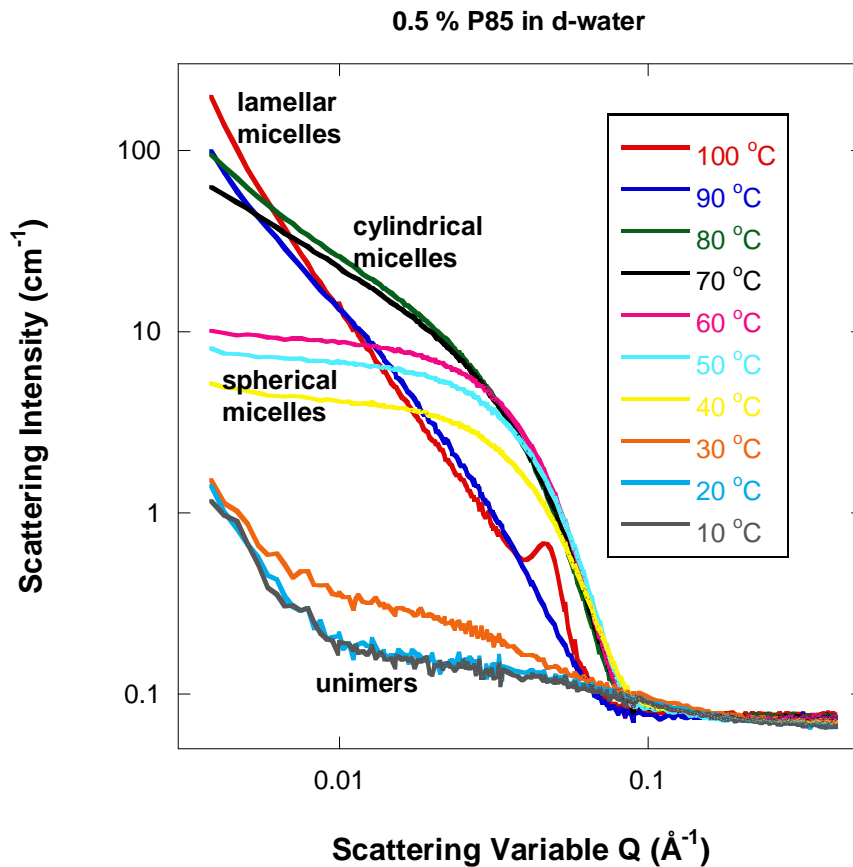


Figure 6: SANS data for the 0.5 % P85 in D<sub>2</sub>O for increasing temperature.

When the PPO central block of P85 becomes hydrophobic, spherical micelles form. Upon heating, hydrogen-bonding between the PEO outer blocks and D<sub>2</sub>O starts softening yielding cylindrical micelles. Upon further heating, the PEO blocks become hydrophobic and lead to a phase transition producing the lamellar structure. In the lamellar phase, the triblock molecules combine to form multilayer structures rich in PEO or PPO; D<sub>2</sub>O is mostly excluded and forms solvent-rich pockets.

A plot of the **low-Q SANS intensity** shows clearly the transition temperatures between the observed phases. Heating and cooling cycles show that these phase transitions are reversible.

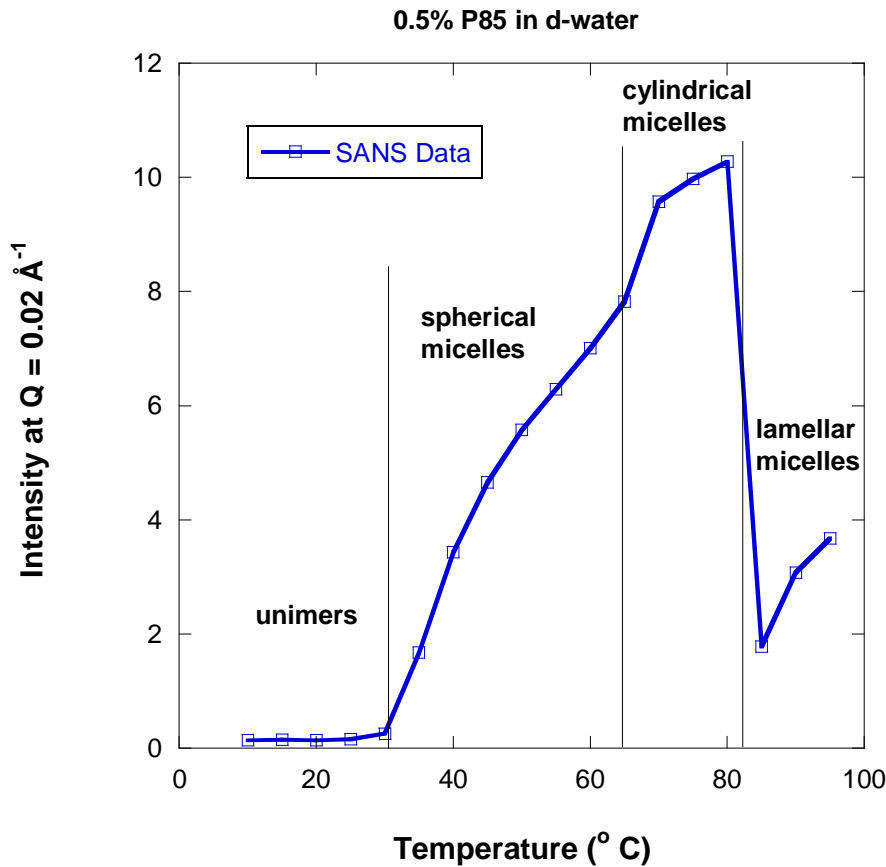


Figure 7: Variation of the low-Q SANS intensity for increasing temperature for the 0.5 % by weight P85/d-water sample.

## 5. THE P85/D-WATER PHASE DIAGRAM

The **P85/d-water phase diagram** has been mapped out (Mortensen, 1996) using the SANS technique (among other techniques). The main phases (**unimers**, **spherical micelles**, **cylindrical micelles** and **lamellar phase**) can be observed at low P85 weight fraction. Other phases (ordered spherical micelles, hexagonal phase and a disordered phase) are not discussed here.

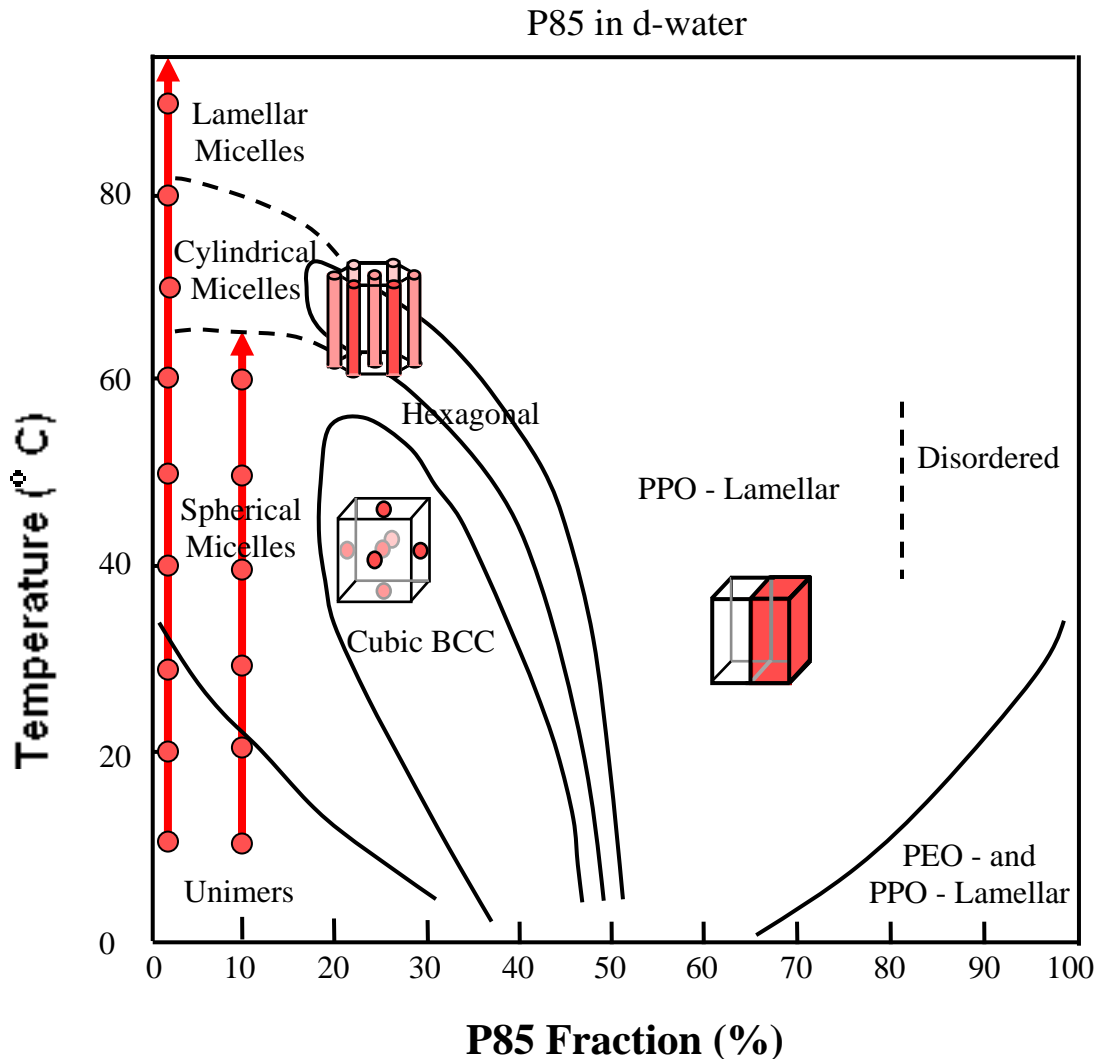


Figure 8: The P85/d-water phase diagram.

## 6. GUINIER-POROD EMPIRICAL MODEL

An empirical generalized Guinier-Porod model is used to analyze the SANS data (Hammouda, 2009). This model describes globular scattering objects (such as unimers or spheres) as well as asymmetric objects (such as rods or lamellae) and uses the following functional form:

$$I(Q) = \frac{G}{Q^s} \exp\left[\frac{-Q^2 R_g^2}{3-s}\right] \text{ for } Q \leq Q_1 \quad (1)$$

$$I(Q) = \frac{D}{Q^m} \text{ for } Q \geq Q_1.$$



The term  $\frac{G}{Q^s} \exp\left(\frac{-Q^2 R_g^2}{3-s}\right)$  is referred to as the Guinier factor. This functional form is

based on the generalized Guinier law for elongated objects. For 3D globular objects (such as spheres),  $s = 0$ , for 2D symmetry (such as for rods)  $s = 1$  and for 1D symmetry (such as for lamellae or platelets)  $s = 2$ . A dimensionality parameter  $3-s$  could be defined.

Applying the continuity of the Guinier and Porod functions and their derivatives at the transition point  $Q_1$  yields:

$$Q_1 = \frac{1}{R_g} \sqrt{\frac{(m-s)(3-s)}{2}} \quad (2)$$

$$D = G \exp\left[\frac{-Q_1^2 R_g^2}{3-s}\right] Q_1^{(m-s)}.$$

This transition at  $Q_1$  is handled internally by the fitting program. This model uses four fitting parameters ( $G$ ,  $s$ ,  $R_g$  and  $m$ ). Nonlinear least squares fits to this model are performed next.

## 7. DATA ANALYSIS USING THE GUINIER-POROD EMPIRICAL MODEL

The empirical Guinier-Porod model is used to analyze SANS data from the 0.5 % P85/d-water at different temperatures. That sample is known to form unimers (dissolved copolymers in solution) at 10 °C, spherical micelles at 50 °C, cylindrical micelles at 70 °C and lamellar micelles at 90 °C. Fits give reasonable results as shown below. The “dimensionality” parameter  $3-s$  varies as it should.

Note that the radius of gyration for a sphere of radius  $R$  is given by  $R_g = R\sqrt{3/5}$ , that for the cross section of an randomly oriented cylinder of radius  $R$  is given by  $R_g = R/\sqrt{2}$ , whereas that for the cross section of a randomly oriented lamella of thickness  $T$  is given by  $R_g = T/\sqrt{12}$ .

Table 1: Results of the fit of the Guinier-Porod model to the SANS data. The reported statistical uncertainties obtained from the fits correspond to one standard deviation.

Temperature	G	3-s	$R_g$ (Å)	m
10 °C	0.032± 0.004	2.75± 0.03	15.81± 0.66	1.53± 0.07
50 °C	8.75± 0.12	3.04± 0.003	47.37± 0.16	4.39± 0.13
70 °C	0.32± 0.003	2.06± 0.002	37.10± 0.14	4.82± 0.16
90 °C	0.0036± 0.0001	1.21± 0.005	27.17± 0.29	2.87± 0.006

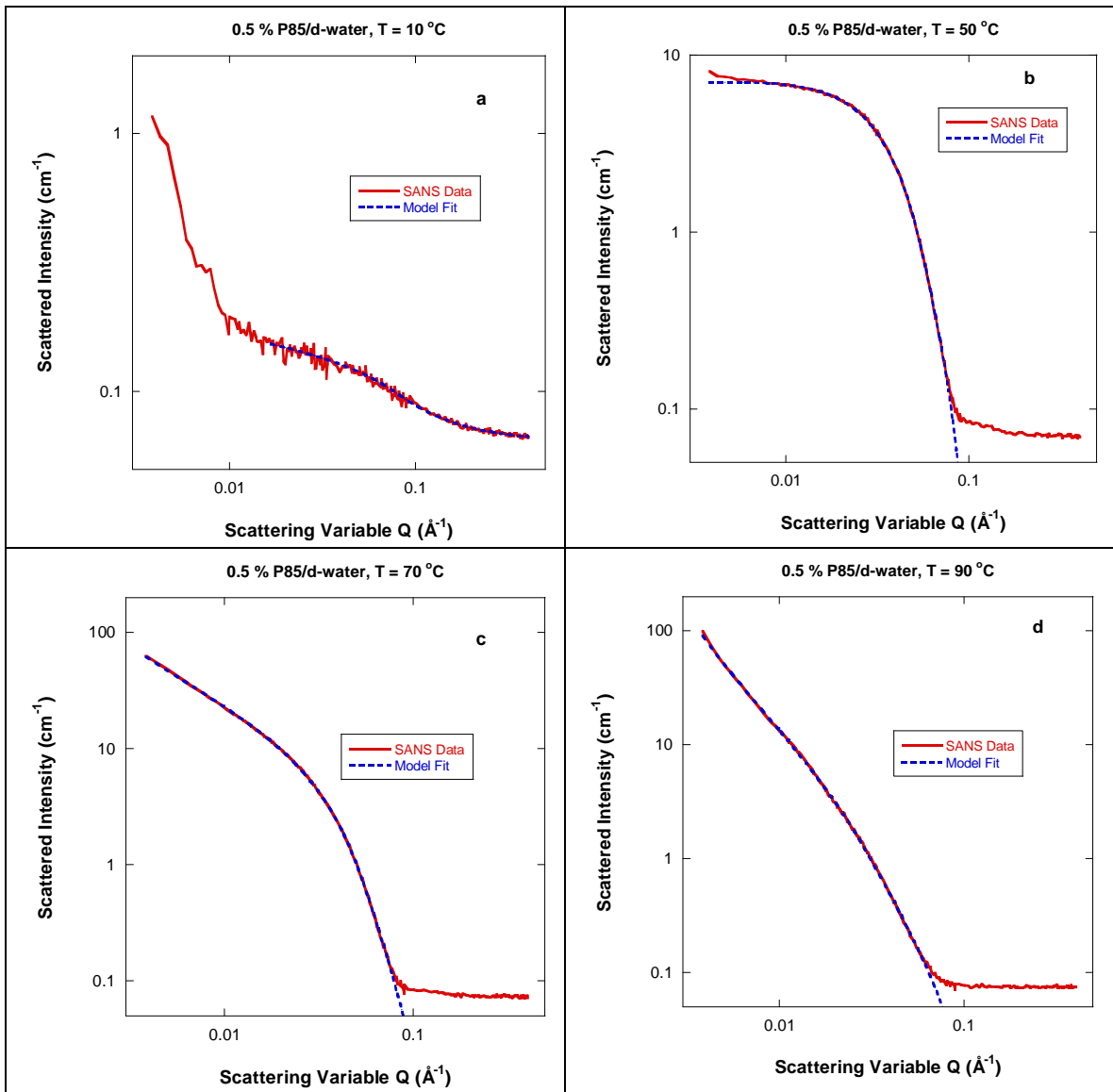


Figure 9: Fits of the generalized Guinier-Porod model to the SANS data from 0.5 % P85/d-water at the various temperatures. (a) Unimers at 10 °C, (b) spherical micelles at 50 °C, (c) cylindrical micelles at 70 °C and (d) lamellar micelles at 90 °C.

Plotting the Guinier factor  $\frac{G}{Q^s} \exp\left[\frac{-Q^2 R_g^2}{3-s}\right]$  yields sharper transitions between the various micellar structures.

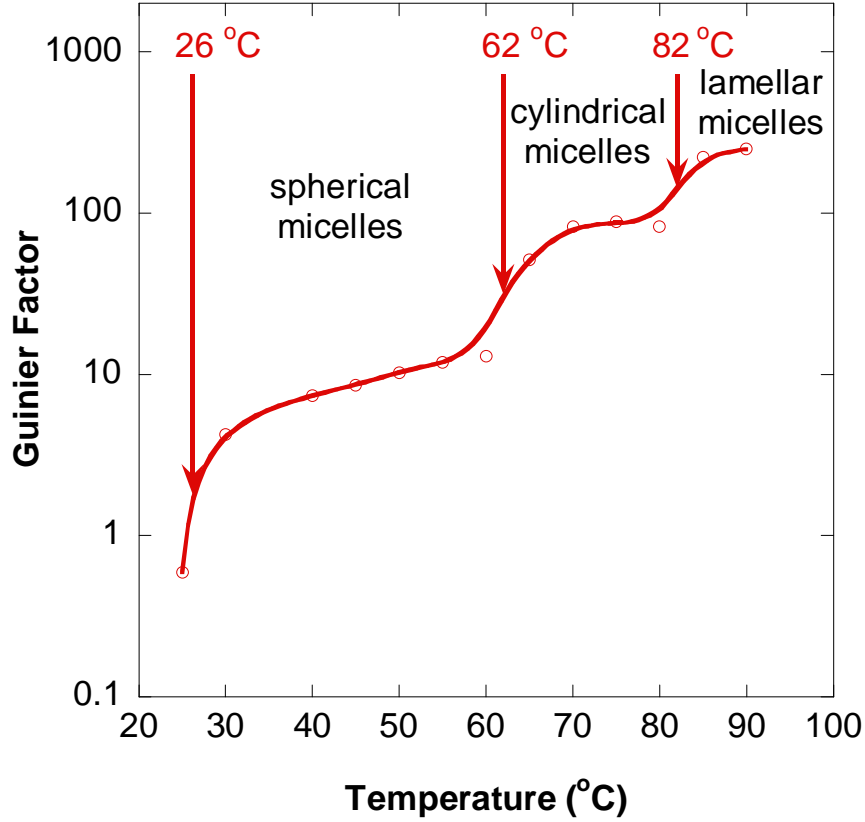


Figure 10: Plot of the **Guinier factor** (first term in Eq. 1) for increasing temperature. Transitions between the various micellar structures are clearly observed.

## 8. MICELLAR STRUCTURES MODELS

At low P85 weight fraction, unimers (dissolved copolymer chains), then spherical micelles, then cylindrical micelles, and finally lamellae form with increasing temperature. These structures are described here. If we assume that the micelles scattering length density is uniform, then **the SANS cross section** (scattering intensity) can be **expressed as follows**:

$$\frac{d\Sigma(Q)}{d\Omega} = \left(\frac{N}{V}\right) \Delta\rho^2 V_P^2 P(Q) S_I(Q). \quad (3)$$

Here  $N/V$  is the micelle number density,  $\Delta\rho^2$  is the contrast factor,  $V_P$  is the micellar volume,  $P(Q)$  is the single micelle form factor and  $S_I(Q)$  is the inter-micelles structure factor.

The **form factor  $P(Q)$  for a Gaussian polymer coil of radius of gyration  $R_g$  is given by the so-called Debye function**:

$$P(Q) = \frac{2}{Q^4 R_g^4} \left[ \exp(-Q^2 R_g^2) - 1 + Q^2 R_g^2 \right]. \quad (4)$$

For a sphere of radius R:

$$P(Q) = \left[ \frac{3j_1(QR)}{QR} \right]^2 = \left[ \frac{3}{QR} \left( \frac{\sin(QR)}{(QR)^2} - \frac{\cos(QR)}{QR} \right) \right]^2. \quad (5)$$

The spherical Bessel function of first order  $j_1(x)$  has been defined.

For a randomly oriented cylinder of length L and radius R:

$$P(Q) = \frac{1}{2} \int_{-1}^1 d\mu \left[ \frac{\sin(Q\mu L/2)}{Q\mu L/2} \right]^2 \left[ \frac{2J_1(Q\sqrt{1-\mu^2}R)}{Q\sqrt{1-\mu^2}R} \right]^2. \quad (6)$$

A lamellar stack of length L and (extended) radius R can also be represented by the same form factor:

$$P(Q) = \frac{1}{2} \int_{-1}^1 d\mu \left[ \frac{\sin(Q\mu L/2)}{Q\mu L/2} \right]^2 \left[ \frac{2J_1(Q\sqrt{1-\mu^2}R)}{Q\sqrt{1-\mu^2}R} \right]^2. \quad (7)$$

Here  $J_1(x)$  is the cylindrical Bessel function of first order.

These models are used to perform nonlinear least squares fits to the SANS data.

## 9. DATA ANALYSIS USING THE MICELLAR STRUCTURES MODELS

Using the relevant IGOR SANS Data Analysis models, fits are performed to the 0.5 % P85/D<sub>2</sub>O SANS data at various temperatures. Since the P85 weight fraction was low, no inter-micelle interactions were considered; i.e., structure factor effects were neglected ( $S_l(Q) = 1$ ) for the unimers, spherical micelles and cylindrical micelles structures. An inter-lamellar structure factor is built into the lamellar structure model considered since lamellae are fundamentally different from other structures. The lamellar phase results from the breaking of hydrogen bonds making PEO blocks hydrophobic.

Since micelle formation is driven by the hydrophobic (PPO) part of the P85 triblock copolymer, core-shell micellar structures are considered in each case (spherical, cylindrical and lamellar). Models that include polydispersity and instrumental smearing effects were used.

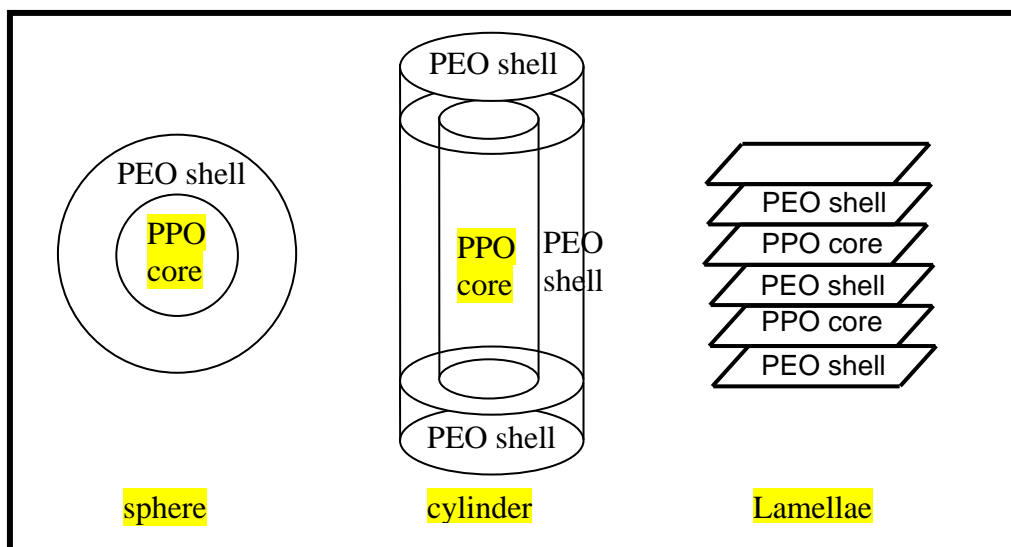


Figure 11: Representation of core-shell sphere, cylinder and lamellar stack.

Using the smeared Debye function model, fits are performed to the 10 °C data. There are three varying parameters: an overall scale factor, a radius of gyration and a Q-independent (mostly incoherent scattering) background. The low-Q SANS upturn characteristic of some form of clustering has been excluded from the fit. The results are included here.

Fit to SmearedDebye,

Data file: X0\_5\_\_p85\_10C\_txt

scale = 0.0871479 ± 0.00092811  
 Rg (A) = 25.397 ± 0.312959  
 bkg (cm-1) = 0.0660033 ± 0.000170499  
 chisq = 349.469  
 Npnts = 191 Sqrt(X^2/N) = 1.35266  
 Fitted range = [28,218] = 0.01393 < Q < 0.3504  
 FitError = No Error FitQuitReason = No Error

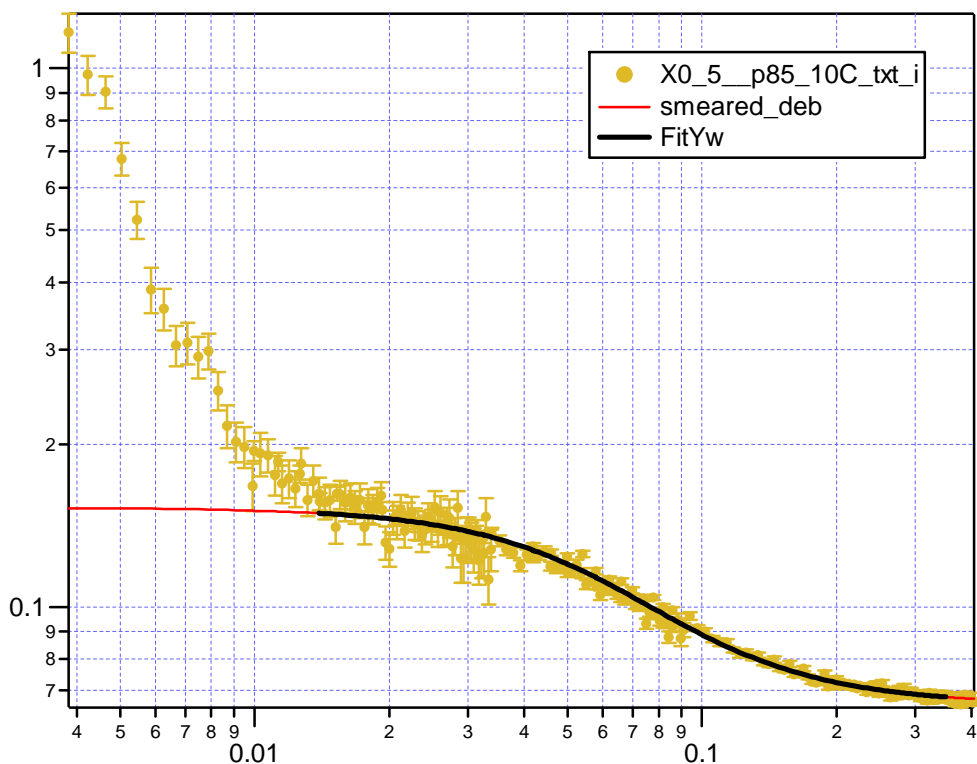


Figure 12: SANS data for the 0.5 % P85/D<sub>2</sub>O at 10 °C and fit to the smeared Debye model.

The smeared polydisperse core-shell sphere model is used to fit the 50 °C data representing spherical micelles. Fitting parameters include an overall scale factor, the sphere core radius and its polydispersity and the shell thickness, the scattering length densities for the core, the shell and the solvent regions and a constant background. The solvent scattering length density is kept constant equal to the value for D<sub>2</sub>O. Note that since the PEO blocks are hydrated, the scale factor is not necessarily equal to the P85 volume fraction.

Fit to SmearedPolyCoreForm,

Data file: X0\_5\_\_p85\_50C\_txt

scale = 0.00883924 ± 0.000177863  
 avg core rad (A) = 46.2927 ± 0.178344  
 core polydisp (0,1) = 0.141087 ± 0.00137233  
 shell thickness (A) = 23.7195 ± 0.479928  
 SLD core (A-2) = 4.38452e-07 ± 1.93293e-08  
 SLD shell (A-2) = 5.58624e-06 ± 3.15427e-08  
 SLD solvent (A-2) = 6.3e-06 ± 0  
 bkg (cm-1) = 0.0706587 ± 0.000121782  
 chisq = 502.904  
 Npnts = 235 Sqrt(X^2/N) = 1.46288  
 Fitted range = [0,234] = 0.003837 < Q < 0.4054

FitError = No Error

FitQuitReason = No Error

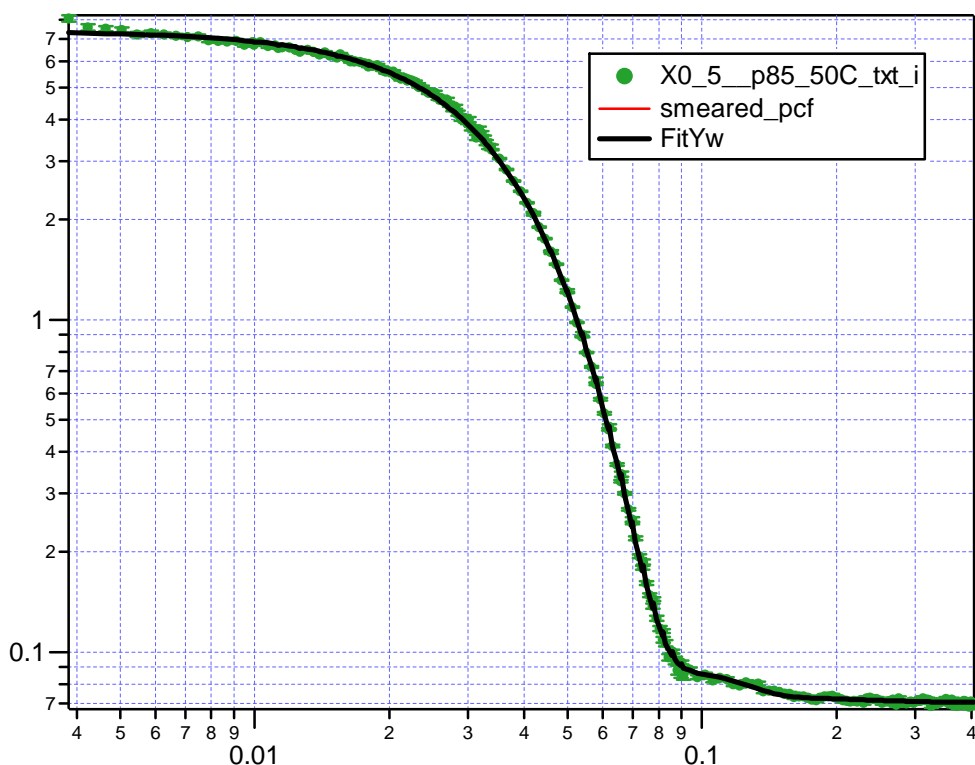


Figure 13: SANS data for the 0.5 % P85/D<sub>2</sub>O at 50 °C and fit to the smeared polydisperse core-shell spherical micelles model.

The smeared polydisperse core-shell cylinder model is used to fit the 80 °C data. The fitting parameters include the scale factor, the mean cylinder core radius and its polydispersity, the cylinder core length, the radial shell thickness and the face shell thickness, the three scattering length densities (core, shell and solvent) and finally the constant background. The solvent scattering length density for D<sub>2</sub>O is fixed during the fits. The numerical integration used to perform the orientational averaging slows down the fitting process. Typical fit results are included.

Fit to SmearedPolyCoShCylinder, 7

Data file: X0\_5\_\_p85\_80C\_txt

scale = 0.0126776 ± 0.627644  
mean CORE radius (A) = 19.2283 ± 0.80576  
radial polydispersity (sigma) = 0.356149 ± 0.0125716  
CORE length (A) = 5770.6 ± 604.38 ← This is a lower bound only  
radial shell thickness (A) = 28.9607 ± 0.790341  
face shell thickness (A) = 1613.72 ± 316.611  
SLD core (A<sup>-2</sup>) = 1.67113e-06 ± 0.000114591  
SLD shell (A<sup>-2</sup>) = 3.74124e-06 ± 6.33398e-05  
SLD solvent (A<sup>-2</sup>) = 6.3e-06 ± 0

incoh. bkg (cm<sup>-1</sup>) = 0.0749588 ± 0.000157727  
 chisq = 1769.76  
 Npnts = 235      Sqrt(X<sup>2</sup>/N) = 2.74425  
 Fitted range = [0,234] = 0.003837 < Q < 0.4054  
 FitError = No Error      FitQuitReason = No Error

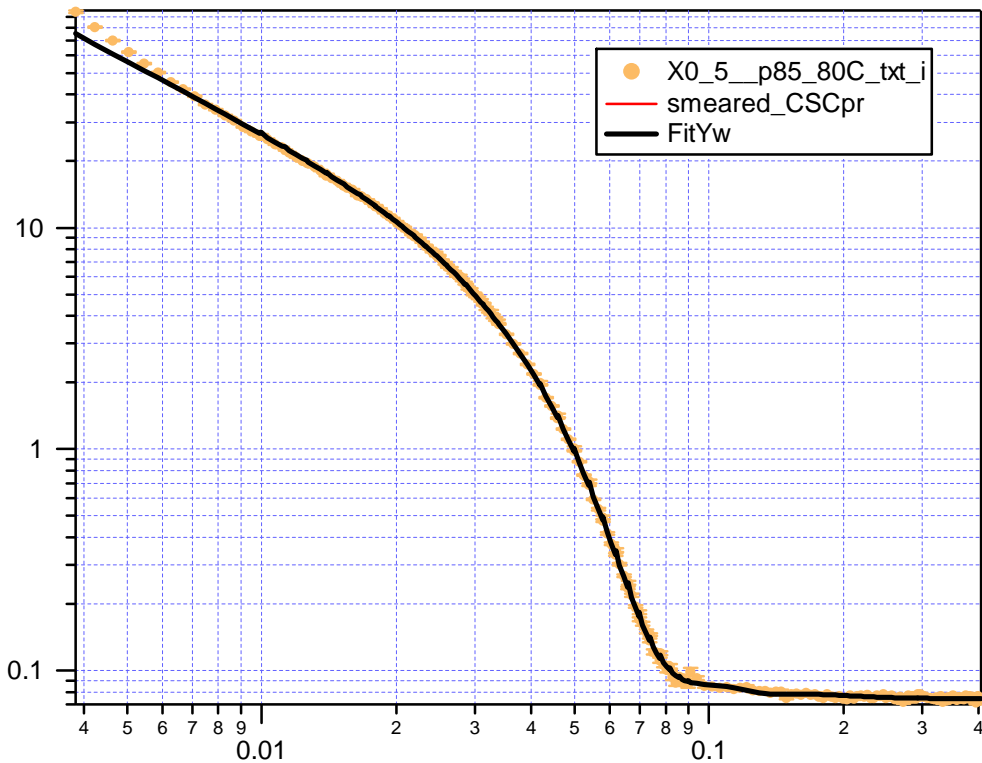


Figure 14: SANS data for the 0.5 % P85/D<sub>2</sub>O at 80 °C and fit to the smeared polydisperse core-shell cylindrical micelles model.

The lamellar structure is harder to model. A crude attempt is included here. Note that this model requires an inter-lamellar structure factor. For the sake of simplicity, details have been left out; some details can be found elsewhere (Hammouda, 200).

This lamellar structure model assumes a stack of lamellae (think of this as a cylindrical stack of disks) with very large disk radius and alternating lamellae (PEO-PPO-PEO, then PEO-PPO-PEO, etc). PEO forms the core part and PEO forms the layer part of the lamellae. This model assumes a small number of lamellae per stack. This model is used to fit the 95 °C data. Fit results are included.

Fit to SmearedStackedDiscs,

Data file: X0\_5\_\_p85\_95C\_txt

scale = 0.0036907 ± 0.363266  
 Disc Radius (A) = 9417.1 ± 0  
 Core Thickness (A) = 34.0089 ± 68.4543



Layer Thickness (A) =  $2.08241 \pm 34.3408$   
 Core SLD (A<sup>-2</sup>) =  $1.79045e-06 \pm 0.000221941$   
 Layer SLD (A<sup>-2</sup>) =  $2.59404e-06 \pm 0.000183072$   
 Solvent SLD (A<sup>-2</sup>) =  $6.3e-06 \pm 0$   
 # of Stacking =  $1.99408 \pm 0.267188$   
 GSD of d-Spacing =  $0.14587 \pm 0.0977305$   
 incoh. bkg (cm<sup>-1</sup>) =  $0.075284 \pm 0.000252143$   
 chisq = 4503  
 Npnts = 228                      Sqrt(X<sup>2</sup>/N) = 4.4441  
 Fitted range = [0,227] =  $0.003837 < Q < 0.3817$   
 FitError = No Error                      FitQuitReason = No Error

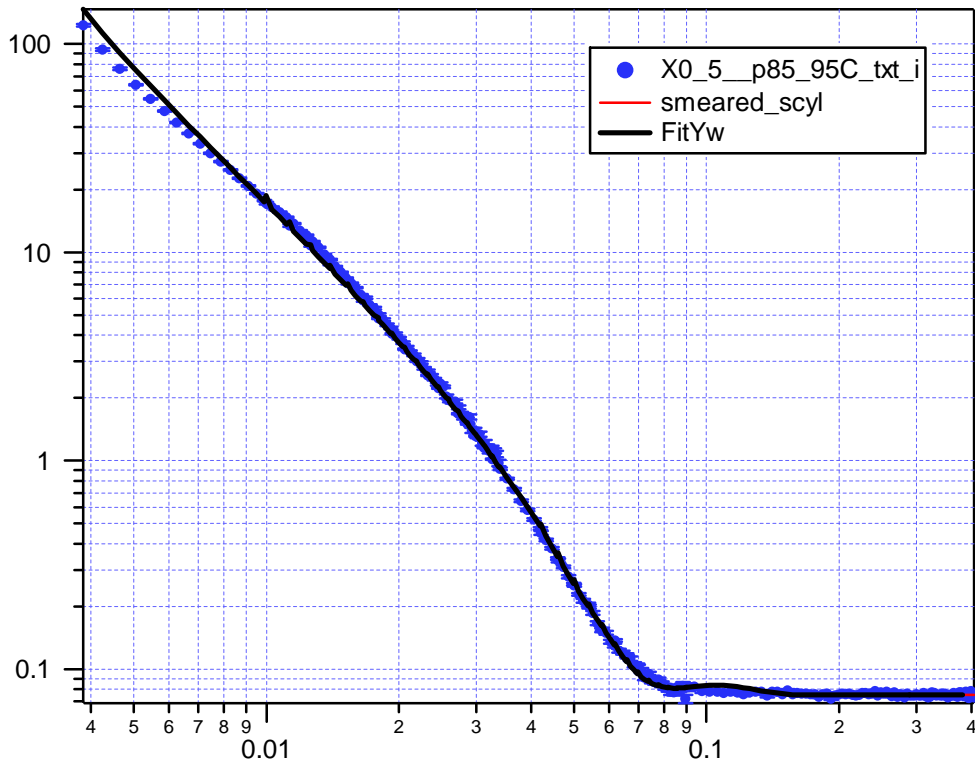


Figure 15: SANS data for the 0.5 % P85/D<sub>2</sub>O at 95 °C and fit to the smeared stacked lamellae model.

This lamellar stack model does not adequately fit the fully developed lamellar structure observed at 100 °C which is characterized by a Bragg peak. This demixed lamellae phase consists of lamellar stacks separated by pockets of solvent. It is formed when the PEO outer blocks demix close to their cloud point temperature.

## REFERENCES

K. Mortensen, “Structural Studies of Aqueous Solutions of PEO-PPO-PEO Triblock Copolymers: Their Micellar Aggregates and Mesophases; A SANS Study” J. Phys.; Condensed Matter 8, A13 (1996).

B. Hammouda, “Probing Nanoscale Structures: the SANS Toolbox”, (2009). This is a book available online at [http://www.ncnr.nist.gov/staff/hammouda/the\\_SANS\\_toolbox.pdf](http://www.ncnr.nist.gov/staff/hammouda/the_SANS_toolbox.pdf). Check for instance chapters 35 and 44.